PARTICLE IDENTIFICATION USING IONIZATION SAMPLING IN THE REGION OF THE RELATIVISTIC RISE

V. Baruzzi,[a] R. Carosio,[b] F. Crijns,[c] L. Gerdyukov,*,[d] Y. Goldschmidt-Clermont,[e] A. Grant,[e] D. Johnson,[f] F. Kröner,[g] I. Lehraus,[e] R. Matthewson,[e] C. Milstene,[h] V. Nikolaenko,*,[d] Y. Petrovikh,*,[d] R. T. Ross,[e] P. Sixel,[i] M. Spyropoulou-Stassinaki,[j] A. Stergiou,[c] W. Tejessy,[e] G. Vassiliadis,[j] P. Wright,[e] J. Zoll[e]

Presented by Y. Goldschmidt-Clermont, CERN

ABSTRACT

Fast secondary particles arising from interactions of K^+ at 70 GeV/c in the BEBC hydrogen bubble chamber, are identified by use of the relativistic rise of ionization in Argon. The ionization is measured in a large multicell proportional counter system, the External Particle Identifier (EPI). Results with identified tracks show the expected separation. The resolution in experimental conditions is studied and compared to that obtained during calibration runs. Individual particles, e.g., secondary kaons are identified at a confidence level of 86%.

Particle identification by ionization sampling in the relativistic rise region is illustrated by preliminary results obtained with the EPI (External Particle Identifier) used in conjunction with the BEBC hydrogen bubble chamber in a study of K^+p interactions at 70 GeV/c. The incident particles from an RF separated beam were tagged before entering the chamber by two multiple finger hodoscopes and two threshold Cerenkov counters. Details about the beam, the bubble chamber and the data reduction methods were published.[1]

A previous publication[2] describes the EPI design and construction methods. It contains results obtained in a calibration run. The EPI consists, essentially, of 4096 proportional counters (cells) of 6x6 cm^2 cross section and 1 m height, stacked in an array of 32 chambers wide and 128 layers deep. The gas used is 95% Ar + 5% CH_4. Each cell is connected to the data acquisition system, a NORD-10 computer, via its individual amplifier and 8-bit ADC. The individual cells and corresponding electronic channels were calibrated during a separate test run using a high energy pion beam. A feedback loop using a β-source irradiating one channel, acted upon the high voltage supply to balance changes due to atmospheric pressure variations. A residual slow time dependent decrease of gas amplification was corrected for in the offline analysis.

The layout of the bubble chamber, the shielding and the EPI is shown on Fig. 1, which also illustrates the pattern of hits in the EPI. The opening in the shielding wall allowed for identification of forward particles only. The low-momentum limit at about 10 GeV/c was imposed by available space and track curvature in the 35 kG BEBC magnetic field.

Positive tracks reconstructed in the bubble chamber were followed through the stray magnetic field of the BEBC magnet to the EPI. Wire chambers were used at approximately mid-distance and attached to the front and back planes of the EPI (not shown on Fig. 1) to assist the tracking. The hit cells of the EPI were associated into strings and these into tracks (over several strings) by a pattern-recognition program, and matched to the bubble chamber tracks. A local cleaning algorithm was developed to localize the cells hit by crossing tracks or other local background (slow electrons, δ-rays, etc.). Overall, the ratio of the number of tracks N_g found with > 50 clean cells ("good" EPI tracks) to the total number N_B of tracks followed from BEBC, through the relatively narrow exit window and into the EPI front plane N_B was $N_g/N_B \approx 0.3$ for $0.15 < X_F < 1$ where X_F is the Feynman scaling variable. The ratio N_g/N_B is practically independent of P_T. As illustrated by Fig. 1, the background was due to crossing tracks arising from secondary interactions in the BEBC exit windows and shielding, and in the EPI frame. Events with excessive background were rejected, they were largely responsible for the losses and for the relatively low value of N_g.

The ionization along the reconstructed tracks was computed from the measurements in each clean cell (corrected by the corresponding calibration values) using the truncated (smaller 40%) mean, with the requirement of ≥ 50 clean cells.

Scatter plots of the ionization versus momentum for subsamples of known tracks are shown on Fig. 2 and Fig. 3. The well identified tracks of Fig. 2 are positive tracks arising from the decay of V^o events identified in the bubble chamber ($K^o \to \pi^+\pi^-$, $\Lambda \to p\pi^-$, $\delta \to e^+e^-$).

The tracks of Fig. 3 are mostly kaons arising from the decay $K^{*o} \to K^+\pi^-$ where the $K^*(890)$ are selected by cuts (viz. $X_F(K^+\pi^-) > 0.8$ and $0.84 < m(K^+\pi^-) < 0.94$), the remaining pion contamination is estimated at ~ 15%.

---

*Participating under the terms of the 1967 Agreement between CERN and the USSR State Committee for the Utilization of Atomic Energy.

a Now at Olivetti S.A., Ivrea, Italy.
b Universita di Genova, Genova, Italy.
c University of Nijmegen, Nijmegen, Netherlands.
d Institute for High Energy Physics, Serpukhov, Protvino, USSR.
e CERN, Geneva, Switzerland.
f Inter-University Institute for High Energy Physics, Brussel, Belgium.
g University of Innsbruck, Innsbruck, Austria.
h Now at Tel-Aviv University, Tel-Aviv, Israel.
i Physikalisches Institut, Aachen, Federal Republic of Germany.
j Now at University of Athens, Athens, Greece.

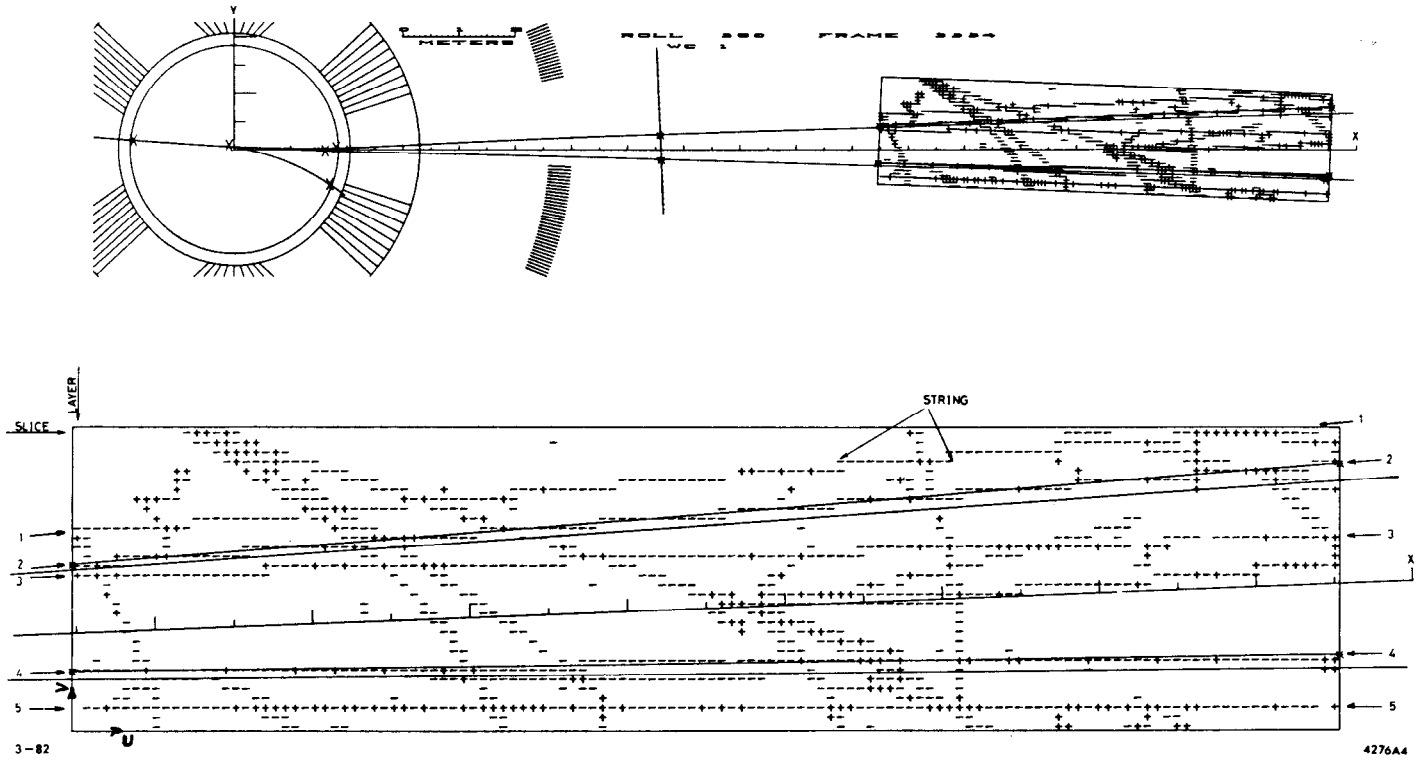

Fig. 1. Top: Layout of the bubble chamber, exit window in the shielding, intermediate MWPC and EPI. A reconstructed event shows tracks followed into the EPI.

Bottom: Pattern of cells hit in the EPI. In addition to the tracks from the reconstructed event, background tracks and secondary interactions are seen.

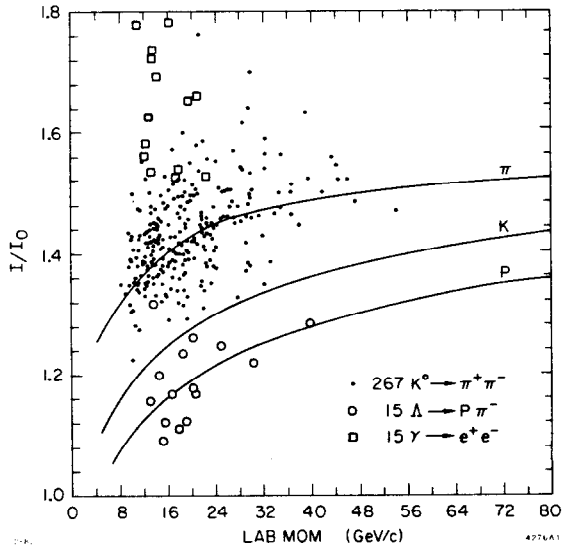

Fig. 2. Ionization vs. momentum for tracks identified by V^0 decays reconstructed in the bubble chamber. The curves are taken from the calibration run.[2]

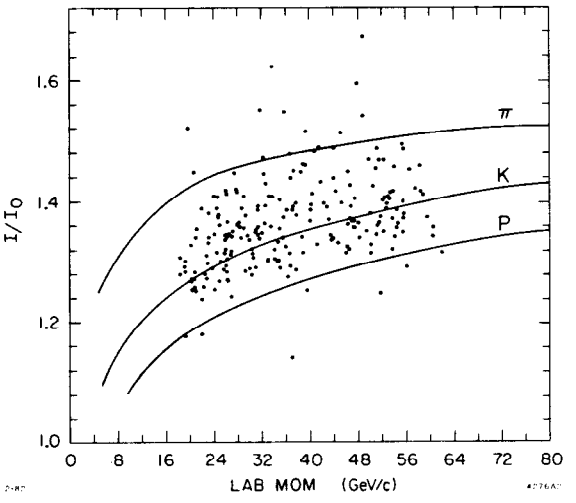

Fig. 3. Ionization vs. momentum for tracks arising from K^* decay (~ 85% kaons). The curves are taken from the calibration run.[2]

The accumulation of points around the expected line for kaons is clearly seen.

A sample of tracks with more than 95 cells, taken amongst all secondaries from interactions in BEBC, is shown on Fig. 4. The accumulation of points corresponding to pions (top) and to kaons (bottom) are visible, as well as the kaons arising from the elastic and diffraction peaks at high momentum. In this plot, the beam-tagging information has been used to remove events arising from a small contamination of the incident beam in protons and deuterons.

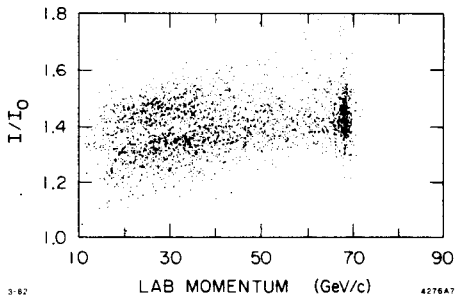

Fig. 4. Ionization vs. momentum for 3071 secondaries of K^+p interactions at 70 GeV/c, for tracks with more than 95 cells. The small beam contamination in protons and deuterons is removed using information from the tagging system.

The distribution of ionization for a sample of tracks where the beam contamination was not removed, and laying in a chosen momentum interval is shown by Fig. 5. It was fitted by three gaussian distributions G_i of the form

$$N(I/I_o) = \sum N_i G_i(\langle \frac{I}{I_o} \rangle_i, \sigma_{G_i})$$

where i = p, K, π and the N_i measures the number of tracks attributed to the p, K, and π populations ($\sum N_i = N$, the number of measured tracks.)

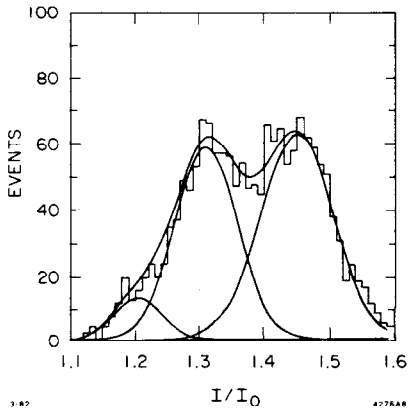

Fig. 5. Distribution of ionization for tracks in the momentum range $22 < p_{LAB} < 28$ GeV/c. The curves are fitted gaussian distributions corresponding to p, K, and π.

The fitted peak values $\langle I/I_o \rangle_i$ are plotted against momentum on Fig. 6, showing a good agreement with the curves obtained from the previous calibration run.[2]

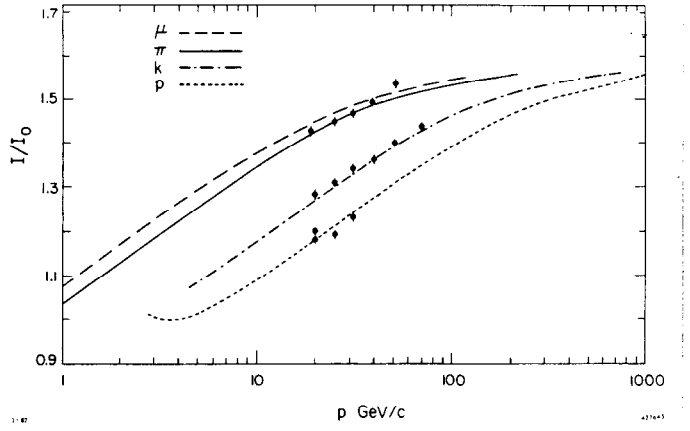

Fig. 6. Average values of ionization as obtained by the gaussian fits vs. momentum. The curves correspond to the calibration values.[2]

The expected width of the gaussian distributions, which gives a measure of the resolution, varies from track to track according to the number n of available clean cells, which depends in turn on the angle of incidence, on the removal of cells during the cleaning process (because of the background due to crossing tracks, δ-rays, etc.). The dependence of the resolution on n, which is roughly of the form $n^{-1/2}$, was determined experimentally on a sample of calibration tracks. In order to estimate the intrinsic width, i.e., the value σ_{128} (n=128) for an ideal track crossing the whole length of the EPI and with ionization measurements in all 128 cells, the following procedure was followed. For several subsamples of tracks, the expected resolution σ_{res} was computed by a convolution of the values for each track i expected from the calibration and the value of n_i. The expected values σ_{res} were compared to the observed values σ_G resulting from the gaussian fit. If the expected σ_{res} were equal to the observed σ_G, they would fall on the diagonal of a scatter plot. The observed values show a slightly degraded overall resolution. This degradation is probably related to such experimental circumstances as residual background, e.g., a not fully efficient filtering of crossing tracks. For tracks with ≥ 50 cells in the momentum region $22 < p_{LAB} < 60$ GeV/c, the gaussian fits give $\sigma \cong 3.8\%$.

The ratios N_i/N with i = p, K, π and $N = \sum N_i$ as defined by the gaussian fits are shown on Fig. 7 as functions of momentum. In this plot, the proton population was not corrected for protons arising as secondaries from interacting beam protons, as may be done by using the tagging information.

Preliminary results based on these measurements were presented at the Notre Dame Conference.[3]

For each measured track, three χ^2 values can be computed as

$$\chi^2_i = \left(\frac{(I/I_o)_{meas} - \langle I/I_o \rangle_i}{\sigma(n)} \right)^2$$

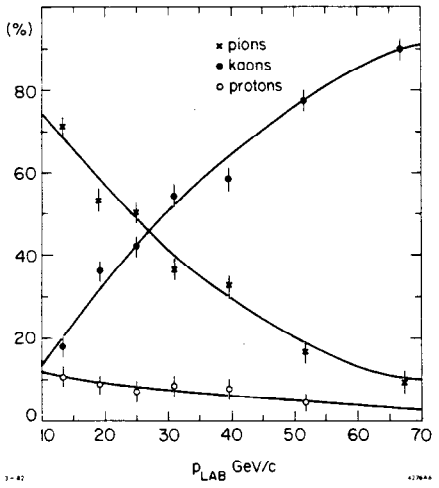

Fig. 7. The populations of p, K, and π amongst secondaries of K^+p interactions at 70 GeV/c as a function of momentum, determined by the gaussian fits. The curves are empirical polynomial fits.

where i = p, K, π (one degree of freedom). The probability that the track be i is then estimated as

$$P_i = \frac{N_i}{N} P(\chi^2_i)$$

where N_i are defined as above. The choice of the highest probability P_i isolates tracks identified as p, K, π. It is estimated, for instance, that the sample of identified kaons contains a contamination of ≤14% of pions. Thus, the individual kaon tracks are identified at a confidence level of 86%.

Similar results are available for an exposure to a RF separated K^- beam at 110 GeV/c.[4] A detailed account of the methods of analysis and of the results is in preparation.

References

1. M. Barth et al., Zeit. Phys. C2 (1979) 285.
2. I. Lehraus, R. Matthewson, W. Tejessy, and M. Aderholz, Nucl. Instr. & Meth. 153 (1978) 347, and
   M. Aderholz, P. Lazeyras, I. Lehraus, R. Matthewson and W. Tejessy, Nucl. Instr. & Meth. 123 (1975) 237.
3. M. Spyropoulou-Stassinaki, Paper presented at the 12th International Symposium on Multiparticle Dynamics, Notre Dame 1981. CERN-EP/81-122, October 1981.
4. P.R.S. Wright, Thesis, Imperial College of Science and Technology, London, 1981.